Experimental Study of Liquid Jet Impingement in Microgravity: The Hydraulic Jump

C.T. Avedisian and Z. Zhao
Sibley School of Mechanical and Aerospace Engineering
Cornell University
Ithaca, New York 14853-7501

Abstract

A preliminary study of the circular hydraulic jump (CHJ) in microgravity is reported using water as the working fluid. The evolution of the CHJ radius was measured during a sudden transition from normal to microgravity in a drop tower. The downstream height of the CHJ was controlled by submerging the target plate in a tank filled with water to the desired depth, and the measurements are compared with an existing theory for the location of the CHJ.

Results showed that the CHJ diameter was larger in microgravity than normal gravity. The adjustment of the CHJ diameter to a sudden change in gravity occurred over a period of about 200ms for the conditions of the present study, and remained constant thereafter. For flow conditions that a CHJ was hot first established at normal gravity but which later appeared during the transition to microgravity, the CHJ diameter was not constant during the period of microgravity but continually changed. Good agreement between the measured and predicted CHJ diameter was found for the normal gravity data, but comparatively poorer agreement was observed for the microgravity measurements.

Introduction

Impingement of a circular liquid jet onto a surface is important in a variety of processes: impingement cooling of electronic devices, materials in manufacturing processes, laser mirrors, and aircraft generator coils; and vapor absorption refrigeration cycles. A feature of impinging liquid jets is their potential for dissipating high heat transfer rates and undergoing a hydraulic jump. Downstream of a CHJ liquid velocity is less than upstream of it and heat transfer is reduced. It is, therefore, important to predict the location of the CHJ and the parameters upon which it depends. Gravity figures prominently in both the location of the CHJ and the abruptness with which the fluid height increases across the jump. The CHJ occurs where the expanding liquid jet undergoes a transition from a 'supercritical' to a 'subcritical' flow, in the the sense of a suitably defined Froude number being greater or less than unity, respectively.

This study is a preliminary effort to improve the understanding of the effect of gravity on a CHJ formed from a laminar circular jet. To isolate the influence of gravity, the fluid and target surface temperatures were the same. Specific objectives were to 1) measure the evolution of a CHJ upon a sudden transition from normal gravity (i.e., $G \equiv g/g_o = 1$ where $g_o = 9.8 m/s^2$) to microgravity ($G \ll 1$), and 2) compare the results with available analyses of jet impingement in microgravity. Existing analyses predict that a CHJ diameter is larger at $G \ll 1$ than at $G = 1$. The present experiment was designed to test this prediction. Measurements were made of the following: 1) evolution of the CHJ radius during the transition from $G = 1$ to $G \ll 1$; 2) the steady state CHJ radius at $G \ll 1$ (also data at $G = 1$ for comparison); and 3) the evolution of the liquid film thickness across the jump during the transition from $G = 1$ to $G \ll 1$. The parameters were the liquid flow rate, jet orifice opening, and the downstream liquid height. The decision to focus on the transition from $G = 1$ to $G \ll 1$ was made because of the available experimental run time of just over 1s.

Brief Review of Related Work

An extensive literature exists on jet impingement in general, and the hydraulic jump in particular. Standard fluid mechanic textbooks provide basic formulations for planar hydraulic jumps (e.g., Allen and Ditsworth 1972; Fox and McDonald 1992). On the CHJ, Nirapathdongporn (1968) reports an extensive search of literature prior to 1968 and reviews the various theories. A number of numerical studies have predicted the behavior of the CHJ in microgravity. At precisely $G = 0$, no jump is predicted (e.g., Thomas et al. 1990). In the vicinity of a jump at $G = 1$, back-flow, separation, and eddies are observed in experimental studies and predicted in early treatements of the problem (e.g., Craik et al. 1981; Tani 1949), but no experimental observations have been reported for $G \ll 1$.

A theoretical analysis by Watson (1964) results in a closed-form solution to the laminar momentum and continuity equations for the CHJ diameter where an inviscid approximation is made for the stagnation region and the flow downstream of the jump, and the flow is self-similar upstream of the CHJ. Some failures of the model are analyzed by Bowles and Smith (1992) who predict the film thickness shape near the jump, and Liu and Lienhard (1993)

who disucss the importance of viscous drag and surface tension. Numerical solutions by Chaudhry (1964) and Higuera (1994) account for the effect of turbulence and heat transfer and provide predictions of both the CHJ diameter and film thickness downstream of the jump.

One experimental study is known on the problem of jet impingement at G<<1 (Labus 1976). The focus was on studying the shapes assumed by a free liquid surface rolling off of the edge of a plate on which the liquid impinges. A drop tower was used to create the microgravity environment. A hint of what to expect for the CHJ diameter at G<<1 was noted by the observation that no CHJ occurred during any of the G<<1 tests while they were a common occurrence at G=1 for nominally the same flow conditions.

Experimental Design

A microgravity environment for the present experiments was created by using a drop tower. Central to the success was the ability to observe all desired features of the flow within the available experimental run time. It was anticipated that the reaction time of the CHJ radius to sudden changes in G would be much less than the available experimental time (on the order of 1s for the facility used). While this was verified for most of the conditions analyzed, for some it was not as discussed in the next section.

The general design of the drop tower used here has been described in past (unrelated) studies (Avedisian et al. 1988; Jackson et al. 1994). It provides for a 7.6m free-fall of an instrumentation package which houses the experiment to give an experimental run time of about 1.25s and a capability for the package to be shielded from air drag. However, the drag shield was not used in this preliminary study for convenience and simplicity of operation. The G value of the unshielded package has a projected maximum after 1.25s of free-fall of about $2.2.2 \times 10^{-2}$ (Avedisian et al. 1988); the shielded package has a maximum G about two orders of magnitude less (Jackson and Avedisian 1994).

A schematic diagram of the apparatus is shown in fig. 1. The components are the following: recirculating pump; plenum containing beads and a flow straightener (to dampen the inlet flow) and a removable orifice plate attached at one end; plexiglas chamber within which the target plate is mounted; flow control valve; and cameras and lighting. The height of the liquid level downstream of the jump is controlled by submerging the target plate to the desired depth by raising the water level above the plate. The experimental conditions examined were the following. The downstream fluid height, h_∞, was 2.0 mm, 4.0 mm, 6.0 mm, 10.0 mm, or 15.0 mm. The liquid flow rates were 2.39ml/s, 6.32ml/s, 9.93ml/s, or 26.47ml/s. To create laminar jets, a sharp-edged orifice was used. Orifice diameters of 1.22mm, 2.56mm and 3.83mm were used. They were machined into a stainless steel plate that could be bolted to the bottom of the plenum. The plenum was mounted such that the orifice was 7.62cm above the target surface. The diameter of the liquid jet, D_j, at a reference $2D_j$ above the target surface was measured directly.

The target plate was a 6.35 mm thick and 23 cm diameter pyrex glass disk painted black on its back to reduce light reflections. A mirror tilted to 45° under the plate allowed for observations of the underside of the jet. Additional viewing angles were along the plane to show the cross-sectional profile shape of the liquid film across the CHJ, and an angled top view for global features of the CHJ. The working fluid was water at room temperature in all the experiments.

To keep the design simple, the primary means of data acquisition was photographic. A 35mm Nikon F3 camera with MD-4 motor drive (operated at 5 frames/s) and attached 105 mm NIKKOR macro lens was used to record images at all three camera positions. Video images using a COHU CCD camera (30 images/s) with attached 28mm NIKKOR macro lens were used to record the evolution of the CHJ in the transition to microgravity. All cameras and lenses were securely mounted to prevent damage due to the shock of the impact. Lighting was provided by halogen lamps. The CHJ diameter was measured from video images of underneath views using a 'video caliper' electronically placed on the vide image. A precision ruler (Schaedler Quinzel, Inc., USA) was added to the image to calibrate (to ±158 μm) the voltage output from the caliper. Side views were used to obtain the cross-sectional shape of the liquid film across the CHJ. The side view images were fed into a MAC-based data acquisition system (AUTOMATIX Image Analysis Program) and an operater-selected gray scale was used to identify the various boundaries involved. A 19.05 mm diameter ball bearing image converted the side view pixel count to length with a precision of about ±66 μm.

Discussion of Results

The response of the CHJ boundary to the transition from G=1 to G<<1 is shown in the representative series of photographs of fig. 2 for a flow rate of $9.6 \times 10^{-6} m^3/s$ and h_∞ = 4 mm for the 2.54 mm diameter orifice opening. The time interval between the photos is about 200 ms and a CHJ initially exists at G=1. In the vicinity of the stagnation point the liquid spreads in a thin film with a smooth surface and then rises abruptly to form a surface roller

in the downstream flow at the CHJ. On the transition to G<<1 (fig. 2b), the liquid boundary at the CHJ appears to be pushed outward; a similar effect occurs at the stagnation point as well where the vertical jet turns and flows horizontally. The mechanism for these effects may be the de-stabilizing effect that G<<1 has on balancing the hydrostatic pressure in the downstream film with the surface tension force on the free surface of the CHJ boundary. At G<<1, the hydrostatic pressure is reduced in the downstream flow and the radius of curvature of the CHJ boundary increases to compensate. This change in curvature of the CHJ boundary creates surface waves at G<<1 in the downstream flow as shown in fig. 2c. Concurrently, the CHJ diameter increases because of the increase in the upstream Froude number caused by the reduction of G.

The profile shape of the liquid across the CHJ during the transition to G<<1 is shown in fig. 3 at five different times after release of the package (at t=0s, G=1) for one flow rate. The dotted line references the target plate. The CHJ boundary was assumed to correspond to the radial position at which the fluid film first increased (note the vertical dotted lines in figure 3) and surface waves first appeared (see fig. 2). The difficulty of identifying the CHJ boundary at G<<1 is evidenced in figs 2 and 3 by the more gradual transition of the CHJ boundary at G<<1 due to the reduction in hydrostatic pressure in the downstream film at G<<1 as noted above.

Fig. 4 shows the evolution of the CHJ radius on the transition from G=1 to G<<1 at two different flow rates for the 2.56 mm diameter orifice and h_∞=4 mm when a jump initially existed at G=1. Fig. 5 shows the evolution when no jump initially existed at G=1 for the 1.22mm orifice and h_∞=15mm. The CHJ diameter was averaged over the time interval of 400ms to 600ms after release of the package. When no jump existed at G=1 (fig. 5), the process of establishing a CHJ at G<<1 was found to first require a brief period in which the liquid near the impingement spot thinned to eventually form the CHJ. Thereafter, the CHJ diameter continuously changed over the entire period of observation (1.25s) as shown in fig. 5, and taking the CHJ diameter in the interval of 400ms to 600ms is more approximate for this case.

Figs. 4 and 5 show that the CHJ diameter increases during the transition to G<<1. The fluid response time to re-establish a new CHJ position after G<<1 is about 200 ms for Q=9.93ml/s and Q=26.47ml/s as shown in fig. 4. The CHJ diameter eventually reaches a constant value at G<<1 within the observation period when a CHJ first existed at G=1, but continuously changes over the entire period of observation when no CHJ existed at G=1. The increase in the CHJ diameter for both cases is due to the increased upstream supercritical Froude number created by a reduction of gravity. In addition, though G continuously increases during the flight of the unshielded package due to air drag (Avedisian et al. 1988), the change was not enough to measurably effect the CHJ diameter after 200ms as shown in fig. 4.

A simplified viewpoint of the origin of a CHJ is that flow of a supercritical expanding film is slowed by friction at the wall and the increasing flow area (due to the radial geometry) until a point is reached at which the flow cannot adjust to the changing downstream conditions because Fr>1 without experiencing a 'jump' in film thickness to satisfy mass conservation. Quantitative developments of the CHJ assume it to be a transition from a flow in which small perturbations are unable to propagate upstream to one in which they are (Higuera 1994). The liquid jet expanding under the influence of an adverse gravitational pressure gradient eventually separates (Tani 1949) as a result of a nonlinear interaction between the wall shear stress, surface tension and the pressure gradient across the film (Bowles and Smith 1992; Gajjar and Smith 1983). This interaction leads to an upstream influence and the CHJ is the result that allows an adjustment of the flow to downstream conditions.

The radial location of the CHJ is most simply determined by assuming a frictionless fluid and applying a mass and momentum balance across a steady CHJ to relate the CHJ diameter, D_h, to the downstream fluid thickness h_∞, the flow rate Q, and the upstream film thickness h as

$$[Q/(\pi D_h)]^2(1/h-1/h_\infty)=1/2g_0(h_\infty^2-h^2)G \qquad 1$$

From eq. 1, D_h can only be determined if h_∞ is known - a motivation for the particular experimental design (fig. 1). As $G\rightarrow 0$, $D_h\rightarrow\infty$ and no jump occurs. Eq. 1 is predictive only in the limit of a high velocity flow. Watson (1964) accounts for viscous effects by using a boundary layer model to predict the velocity profile across the upstream film and finds that the flow becomes self-similar at some radial position away from the stagnation point. This theory has the essential features of more advanced treatments (e.g., Bowles and Smith 1992; Higuera 1994) and is applied to the present data. The modification of eq. 1 due to Watson (1964) for the case of a boundary layer that covers the entire film can be expressed in non-dimensional form as (Middelman 1995)

$$Y = .26/(R^3+.287) \qquad 2$$

where $Y \equiv RH/Fr_\infty + 1/(2RH)$, $R \equiv D_h/D_j Re^{-1/3}$, $Re \equiv 4Q/(\pi D_j \nu)$, $H \equiv 2h_\infty/D_j\ Re^{1/3}$, $Fr_\infty r \equiv U_j^2/(G\ g_0 h_\infty)$ and the approximation $h_\infty >> h$ has been made. The inviscid limit is $R \rightarrow 0$ in eq. 2. Y and R are known from the experimental results: D_h as discussed previously, and h_∞ and Q as input parameters ($U_j = Q/[\pi D_j^2/4]$). A reference location of $2D_j$ above the target surface was used to measure D_j. For the water kinematic viscosity at 300°K, $\nu \approx 8.95 \times 10^{-7} m^2/s$ (Keenan et al. 1969). An average G of 1.1×10^{-2} is used over the free-fall distance.

Fig. 6 shows the variation of Y with R. The inviscid limit (dotted line) clearly does not predict any of our measurements (a not unexpected result (Watson 1964)). All of the G=1 data are predicted reasonably well when viscosity effects are included (eq. 2). This agreement suggests that for the experimental parameters examined the conditions of Watson's analysis are reasonably well satisfied in the experiments, for example the neglect of viscous drag at the plate and the boundary layer being fully developed in the film. On the other hand all of the measurements of D_h for $G << 1$ show poorer agreement with eq. 2. This result may indicate a number of possibilities, including that some process not included in the development of eq. 2 becomes important at $G << 1$. Candidates include flow separation downstream of the jump and the nonuniform downstream velocity, neglect of viscous drag at the surface of the plate, or surface tension, in addition to uncertainties in identifying the CHJ boundary at $G << 1$ noted above.

Conclusions

Experimental measurements of the CHJ in microgravity showed the following results for the particular experimental conditions examined: 1) a steady CHJ can be established in microgravity; 2) the CHJ in microgravity is larger than at normal gravity, other flow conditions being the same; 3) the fluid response time during the transition to microgravity is on the order of 200ms when a jump exists at normal gravity; 4) when flow conditions are such that a CHJ does not exist at normal gravity, the fluid response time appears to be greater than 1s after the transition to microgravity; 5) the film thickness across the CHJ boundary at $G << 1$ is more gradual due to the reduction in hydrostatic pressure in the downstream film; and 6) the G=1 measurements are well correlated by an existing formulation but the microgravity measurements show comparatively poorer agreement.

Acknowledgments

The authors wish to thank the Microgravity Science and Application Division of NASA for supporting this preliminary study. Thanks go to Dr. David Chao of NASA for serving as technical monitor and for his encouragement throughout the course of this study, and to Mr. Jack Salzman of NASA for drawing to the authors' attention the reference to Labus (1976). The assistance of Messrs. Jun-Eu Tang and Hanwook J. Kim of Cornell in performing some of the experiments is appreciated.

REFERENCES

Allen, T. and Ditsworth, R.L. (1972) *Fluid Mechanics*, pp. 291-291, McGraw-Hill, New York.
Avedisian, C.T., Yang, J.C and Wang, C.H. (1988) *Proc. R. Soc. Lond* A**420**, 183.
Bowles, R.I. and Smith, F.T. (1992) *J. Fluid Mechanics.* **242**, 145.
Chaudhury, Z.H. (1964) *J. Fluid Mechanics.* **20**, 501.
Craik, A.D.D., Latham, R.C., Fawkes, M.J. and Gribbon, P.W.F. (1981) *J. Fluid Mechanics* **112**, 347.
Fox, R.W. and McDonald, A.T. (1992) *Introduction to Fluid Mechanics*, 4th edition, pp. 525-530, John Wiley, New York.
Gajjar, J.S.B. and Smith, F.T. (1983) *Mathematika* **30**, 77.
Higuera, F.J. (1994) *J. Fluid Mechanics.* **274**, 69.
Jackson, G.S. and Avedisian, C.T. (1994)*Proc. R. Soc. Lond.*, A**446**, 257-278.
Keenan, J.H., Keys, F.G., Hill, P.G., and Moore, J.G. (1969) *Steam Tables* , p. 114, John Wiley, New York.
Labus, T.L. (1976) "Liquid Jet Impingement Normal to a Disk in Zero Gravity," Ph.D. Thesis, University of Toledo.
Liu, X. and Lienhard, J.H. (1993) *Exp. Fluids*, **15**, 108.
Middelman S. (1995) *Modeling Axisymmetric Flows*, Chapter 5, New York, Academic Press.
Nirapathdongporn, S. (1968) "Circular Hydraulic Jump", M.Eng. Thesis, Asian Institute of Technology, Bangkok, Thailand.
Thomas, S., Hankey, W.L., Faghri, A., and Rahman, M.M. (1990) *J. Heat Transf.* **112**, 728.
Tani, I. (1949) *J. Phys. Soc. Japan* **4**, 212.
Watson, E.J. (1964) *J. Fluid Mechanics* **20**, 481.

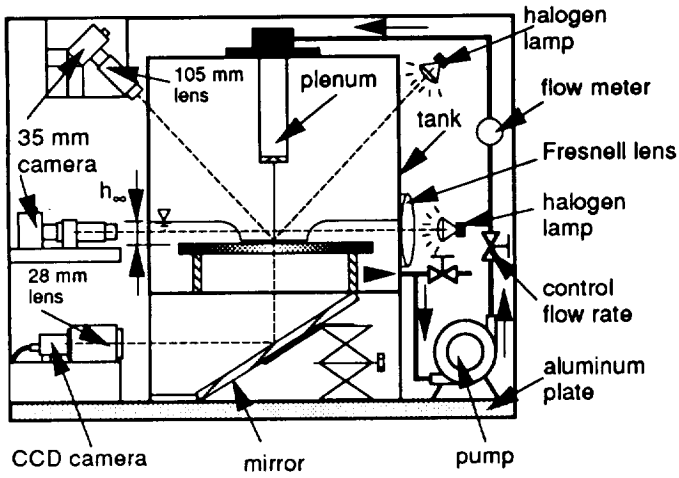

Figure 1

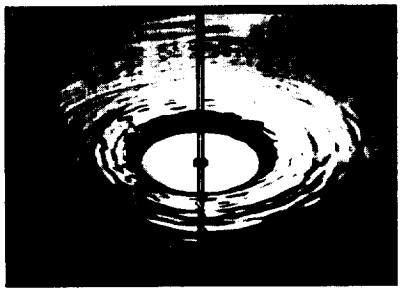

t=0, G=1

Figure 2a

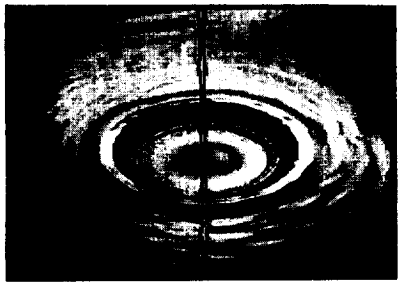

20 mm

t=200 ms, G<<1

Figure 2b

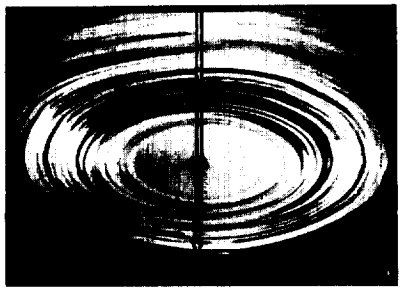

t=400 ms, G<<1

Figure 2c

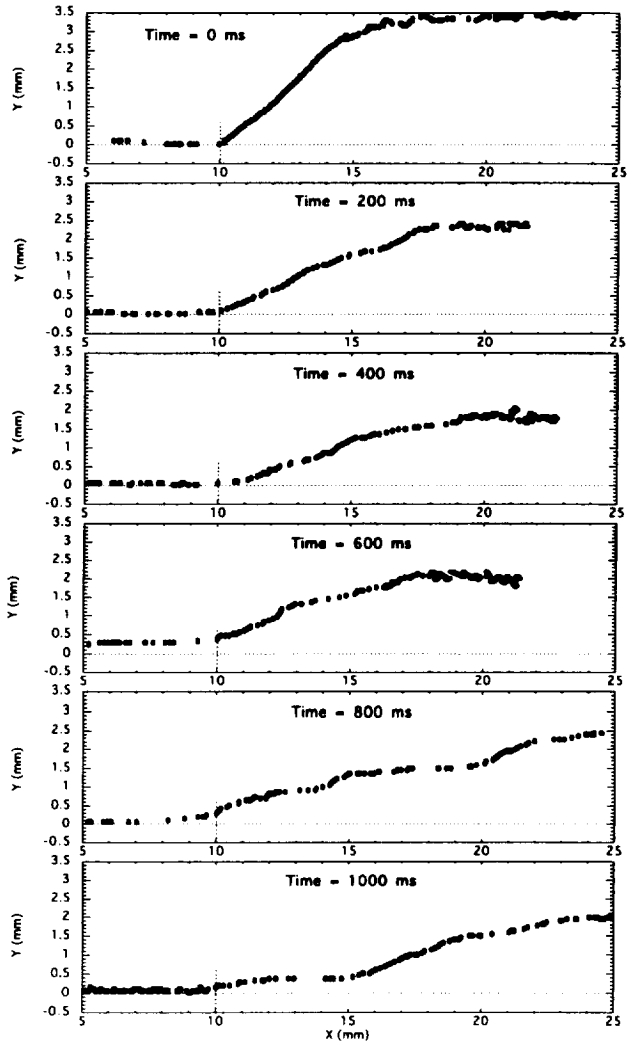

t=0, G=1; t>0, G<<1

Figure 3

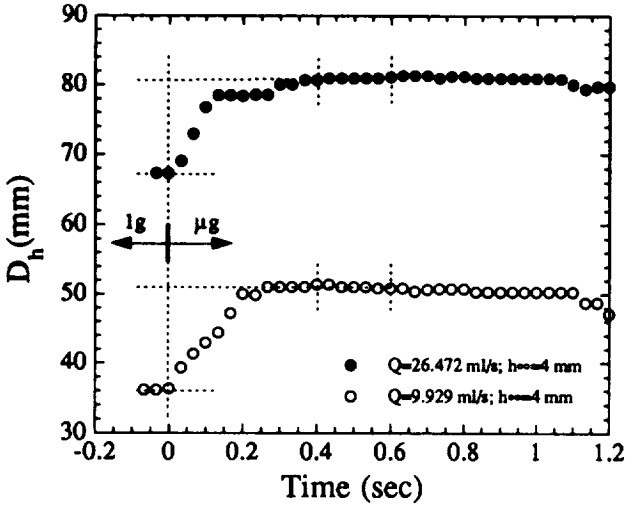

Figure 4

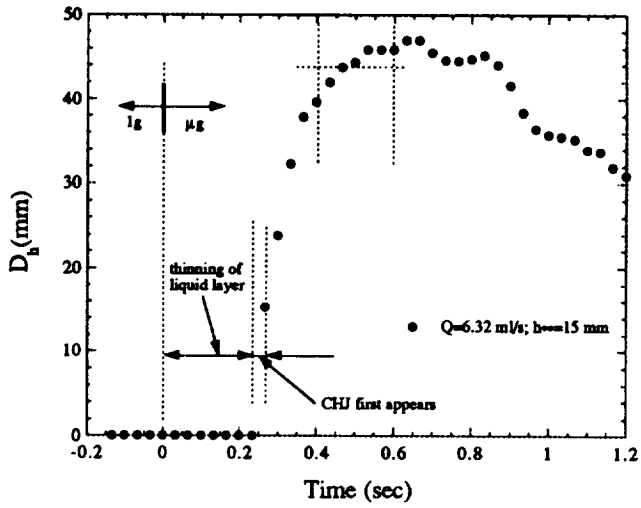

Figure 5

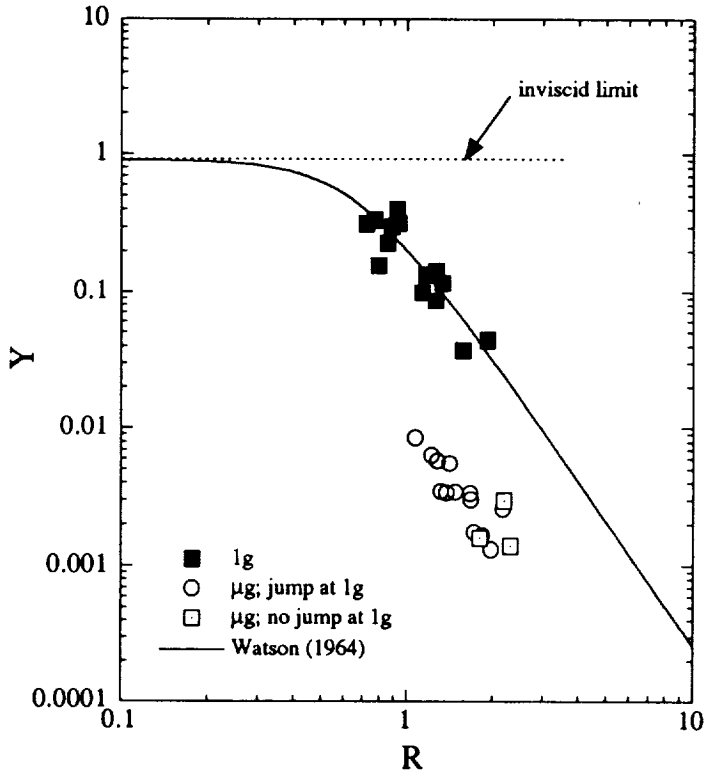

Figure 6